PCCP

Accepted Manuscript

ROYAL SOCIETY OF CHEMISTRY

www.rsc.org/pccp

Exploring the mechanism of water-splitting reaction in NiO_x/β-Ga_2O_3 photocatalyst by first-principles calculations

Xin Zhou[a]*, Hao Dong[b], and Ai-Min Ren[c]

a College of Environment and Chemical Engineering, Dalian University, Dalian 116622, China. E-mail: zhouxin@dlu.edu.cn

b Institute of Chemistry for Functionalized Materials, School of Chemistry and Chemical Engineering, Liaoning Normal University, Dalian, Liaoning 116029, China.

c State Key Laboratory of Theoretical and Computational Chemistry, Institute of Theoretical Chemistry, Jilin University, Changchun 130023, China

Abstract

Experiments found that loading suitable cocatalysts, usually in the form of metal and metal oxide nanoparticles, on the semiconductor surface can remarkably increase the photocatalytic activity of water-splitting reaction. To get insight into the mechanism of experimental observations, we took NiO_x/β-Ga_2O_3 photocatalytic system as a model and performed detailed density functional theory calculations. Electrochemical computational methods are used to investigate the hydrogen evolution reaction (HER) and oxygen evolution reaction (OER). Our results show that in Ni_4O_2/β-Ga_2O_3 system, the reaction sites of HER are on cluster oxygen atoms and Ni atoms in Ni_2 cluster. Loading Ni_4O_2 cluster on β-Ga_2O_3 surface importantly reduces the reaction free energy of HER. On the clean β-Ga_2O_3 surface, water dissociation is energetically unfavorable. After attaching Ni_4O_2 cluster to the surface, water decomposition becomes thermodynamically favorable. The favorable reaction sites of OER focus on Ni_4O_2 cluster. The rate-determining step of OER can be changed by adsorbing Ni_4O_2 cluster. Notable reduction of overpotential (0.87 V) for OER on Ni_4O_2/Ga_2O_3 is found compared with that on clean Ga_2O_3 surface, which reasonably explains the experimental observation on significant enhancement of activity for generating oxygen after loading NiO_x cocatalysts.

1. Introduction

Being considered one of the most attractive approaches to solving energy and environmental issues at a global level, photocatalytic water-splitting is drawing increasing attention, mainly from academia.[1-5] In general, a heterogeneous photocatalyst system is composed of semiconductor and cocatalysts.[6] The semiconductor is responsible for harvesting light, while photocatalytic reactions take place on cocatalysts loaded on the semiconductor. Cocatalysts could serve as reaction sites, catalyze reactions, and promote the charge separation and transport driven by junctions/interfaces formed between cocatalyst and light harvesting semiconductor.[7] The overall water splitting reaction is a thermodynamically uphill reaction involving multiple electron transfer processes, which includes two half reactions, hydrogen evolution reaction (HER) and oxygen evolution reaction (OER). Many research studies show that loading proper cocatalysts on the light harvesting semiconductor could promote or accelerate the photocatalytic courses of HER and OER. [8-12] Typically, the cocatalyst is a noble metal for HER (such as Pt, Pd, Ru, Rh and Au) or transition-metal oxide for OER (such as CoO_x, NiO_x, IrO_2, MnO_x and RuO_2).

Among so many developed materials, photocatalytic systems that are capable of simultaneously reducing and oxidizing water are very rare.[13] Nickel oxide loaded gallium oxide (Ga_2O_3) is one of the few materials that can achieve the reaction in pure water, without the need for expensive platinum group elements.[14-18] In general, the pretreatment of H_2 reduction and subsequent O_2 oxidation is indispensable for the nickel oxide loaded photocatalysts to show high activities. One can imagine that this

kind of nickel oxide should be a mixture of Ni and NiO nanoparticles, which is often denoted as NiO_x in the literature.[14-20] The results reported by Yanagida *et al.* show that only H_2 production was observed when Ga_2O_3 was used as the photocatalyst without NiO_x loading, and the activity was relatively low.[14] A recent work showed that NiO_x loading is necessary to induce the stoichiometric formation of H_2 and O_2 by photocatalytic decomposition of water on Ga_2O_3 with tunable α-β phase junctions.[16]

Cocatalysts are typically present as nanoparticles on the semiconductor surface loaded by impregnation or *in situ* photo-deposition.[21] The structural complexity of the nano-sized metal or metal oxide clusters on semiconductor surfaces makes it difficult to obtain structural and electronic information for these systems even under well-defined experimental conditions. Theoretical studies based on first-principles electronic structure calculations have proven to be useful for complementing the experimental results to illuminate the relationship between the surface structure and the physical and chemical properties of semiconductors, and further to understand the mechanism of photocatalytic reaction.[22-29]

Although experimental observations indicate that cocatalysts play an important role in providing reaction sites and increasing activity in photocatalytic systems, several critical questions on cocatalysts are still open. For instance, what is the existence form of cocatalysts on the surface of semiconductors? How does the adsorption of cocatalysts affect the electronic properties of photocatalysts? Why does loading cocatalysts promote the charge separation? What is the mechanism of photocatalytic water-splitting reaction in such complex material systems? In this regard, we

previously took the Ni-NiO/β-Ga_2O_3 as the model and used DFT calculations to study small Ni_n and Ni_nO_n (n=1-4) clusters adsorbed at the β-Ga_2O_3(100) surface.[30] In that study we found that small Ni_n and Ni_nO_n clusters tend to formed on different sites of the surface, which is favorable for the charge separation. The electronic structure analyses indicate that Ni_n/Ga_2O_3 systems participate in the photocatalytic HER while Ni_nO_n/Ga_2O_3 systems tend to take part in the photocatalytic OER. In this work, in order to approach realistic experimental conditions, we have performed calculations on the Ni_4O_2 cluster, a mixture of Ni_2 and Ni_2O_2, to simulate NiO_x supported on the β-Ga_2O_3 surface. Based on the determined stable configurations and electronic structures for Ni_4O_2 adsorbed on the β-Ga_2O_3 surface, we explored water adsorption on semiconductor surface and the mechanism of the water-splitting reaction in the NiO_x/Ga_2O_3 photocatalytic system.

2. Computational Details

All the DFT spin-polarized calculations were performed with the VASP (Vienna Ab initio Simulation Package) code.[31,32] The exchange correlation potential was described through the Perdew-Burke-Ernzerhof (PBE) functional within the generalized gradient approximation (GGA) formalism.[33] The projector-augmented wave method was applied to describe electron-ion interactions.[34,35] Different methods have been used to correct the self-interaction errors arisen from conventional semi-local functionals depending on the studied systems, such as DFT+U,[36-39] hybrid functionals, [40-42], and linear response approaches.[43,44] In this work, A Hubbard *U* term acting on the Ni 3d orbitals was added to the standard PBE functional employing the

rotationally invariant formalism developed by Dudarev et al.,[36] in which only the difference (U_{eff} = U - J) between the Coulomb U and exchange J parameters is considered. In the present work, a value of U_{eff}=5.3 eV was used, which was calculated self-consistently by Ferrari *et al.*[37] and which is in the range of 5-6 eV interval found in the literature.[36,38,39]

Among the five different crystalline structures of Ga_2O_3, β-Ga_2O_3 is the most stable crystal phase.[45] This crystal phase exhibits excellent photocatalytic activity,[46,47] and it is the subject of extensive experimental and theoretical studies.[48-54] Full optimization of the cell parameters for the bulk β-Ga_2O_3 with monoclinic structure was carried out by using the 3×11×7 Monkhorst-Pack type *k*-point sampling. The cutoff energy for the plane wave basis set was fixed at 520 eV. The calculated lattice parameters, a=12.504 Å, b=3.101 Å, c=5.915 Å, and β=103.71°, are in good agreement with the experimental data.[55] A (3×2) supercell including a cell composition of $(Ga_2O_3)_{24}$ was used to simulate the (100)-B surface of β-Ga_2O_3, which is the most stable one among five surfaces studied by experimental and theoretical works.[56-58] For all the surface calculations, a vacuum layer of 15 Å was used in order to avoid the interaction between periodic slabs. The valence electrons are described by a plane wave basis set and the cut-off for the kinetic energy is 400 eV. For the Brillouin zone integration, a Monkhorst-Pack set of 3×3×1 *k*-points was applied. The upper half of the slab and the adsorbates were allowed to relax, while the bottom half of the slab was fixed at its optimized bulk position. Dipolar corrections were included along the axis normal to the surface. The geometries were considered to be converged when the forces on each

ion were less than 0.01 eV/Å.

On top of the optimized geometries obtained at the GGA-PBE level, a more accurate approach, the hybrid HSE06 functional,[40-42] was used to calculate the electronic properties for the most stable structure. This is necessary in order to achieve a good agreement between the experimental and the theoretical band gaps. The HSE06 functional includes a fraction α, of screened, short-range HF exchange to improve the derivative discontinuity of the Kohn-Sham potential for integer electron numbers. The percentage of HF exchange in a hybrid functional is not a universal constant and the optimal value can be system-dependent. The band gap of bulk β-Ga_2O_3 was obtained from experiments to be in the range of 4.2-4.7 eV. [16,47,59,60] In the present work, an α=0.3 was used as this value can yield a good agreement between the computed band gap (4.5 eV) and the experimental results.

3. Formation of Ni_4O_2 clusters on (100)-B surface of β-Ga_2O_3

In order to obtain the most stable structure for adsorbing Ni_4O_2 cluster on the β-Ga_2O_3(100) surface, a lot of initial configurations were motivated by the work of Jacob's group and considered by starting from different sites and orientations,[61] such as adding two oxygen atoms to the most stable structure of Ni_4/β-Ga_2O_3(100), adding two nickel atoms to the favorable structure of Ni_2O_2/β-Ga_2O_3(100).[30] Fig. 1 displays fifteen optimized structures and relative energies with respect to the lowest-energy structure. There are four structures with similar stability, since the relative energy to the most stable configuration is within 0.02 eV. Here we only focus on the lowest-energy structure to present the following discussions. Key structural

parameters for the most stable configuration are shown in Fig. 2. As we can see from the figure, the most favorable structure of Ni_4O_2/β-Ga_2O_3(100) is composed of the most stable structures of Ni_2/β-Ga_2O_3(100) and Ni_2O_2/β-Ga_2O_3(100) with some distortions. In comparison with the relaxed structures of Ni_2/β-Ga_2O_3(100) and Ni_2O_2/β-Ga_2O_3(100), the change of the bond lengths for Ni_2 moiety and Ni_2O_2 moiety in Ni_4O_2/β-Ga_2O_3(100) is within 0.02 Å and 0.05 Å, respectively. The arrangement of Ni atoms in Ni_2 cluster on the surface is changed since new Ni-O and Ni-Ni bonds formed. In this work, the adsorption energy, E_{ads}, of a cluster adsorbed on the β-Ga_2O_3(100) surface was defined as:

$$E_{ads} = E_{total} - E_{surface} - E_{cluster} \quad (1)$$

where E_{total} is the total energy of the Ga_2O_3 surface with a cluster, $E_{surface}$ is the total energy of the bare and relaxed surface, and $E_{cluster}$ is the energy of optimized cluster in the gas phase. Based on Equation (1), we have calculated the adsorption energy of Ni_2O_2 cluster on Ni_2/β-Ga_2O_3(100) surface and the one of Ni_2 cluster on Ni_2O_2/β-Ga_2O_3(100). The former is computed to be -6.79 eV and the latter is predicted to be -5.59 eV. Both processes are exothermic, that is to say, the formation of NiO_x on Ga_2O_3 is energetically favorable.

On the basis of the relaxed structures, we have analyzed the TDOS and PDOS of clean β-Ga_2O_3(100) and Ni_4O_2/β-Ga_2O_3(100) surfaces by means of HSE06 method. As shown in Fig. 3(a),[30] the valence band maximum (VBM) is mainly composed of O 2p states, slightly hybridized with Ga 3d and 4p states. Ga 4s states contribute more to the lower valence bands. The conduction band minimum (CBM) consists mostly of

Ga 4s states. The valence bands exhibits the characteristic of mixed O 2p, Ga 4s, 4p and 3d states. The strong mixing of O and Ga orbitals is indicative of the high degree of covalent bonding in this semiconductor. The value of band gap is computed to be 4.0 eV, which is smaller than that of the bulk (4.5 eV) due to the surface dangling bonds. Fig. 3(b) indicates that the effect of adsorbing Ni_4O_2 cluster on the electronic structure. Several impurity states from Ni_4O_2 cluster appear in the band gap of Ni_4O_2/β-Ga_2O_3(100). Due to a bond formed between O atom and the Ni atom in Ni_2 cluster, there is a considerable overlap between O 2p states and Ni_{Ni2} 3d states just below the Fermi level. As shown in Fig. 3(b), most of cluster O 2p states and Ni 3d states in Ni_2 cluster are near to or located in VBM, which is well mixed with surface O 2p states and Ga 3d states. The occupied Ni 3d states in Ni_2O_2 cluster are mainly situated in the valence bands within the range of -7 to -2 eV, which overlap with Ga 4s and Ga 4p states as displayed in Fig. 3(a). While the unoccupied Ni 3d states in Ni_2O_2 cluster contribute the lower conduction band and mix with Ga 4s states.

In order to investigate the charge distribution at the interface between Ni_4O_2 cluster and the Ga_2O_3 surface, we have performed Bader charge analyses on Ni_4O_2/Ga_2O_3. The calculated results show that after adsorbing on Ga_2O_3 surface, the total charge of Ni_2 moiety and Ni_2O_2 moiety is +0.70 and -0.31, respectively. In the Ni_2O_2 fragment, Ni_2 shows positive charge (+0.99) and O_2 shows negative charge (-1.30). This indicates that the charge flow occurs from Ni atoms to surface O atoms, and from surface Ga atoms to cluster O atoms simultaneously.

4. The mechanism of water-splitting reaction on Ni_4O_2/β-Ga_2O_3(100)

In this section, we took Ni_4O_2/β-$Ga_2O_3(100)$ as the model to investigate the reaction site and mechanism of HER and OER in NiO_x/Ga_2O_3 photocatalyst. We only focus on the thermodynamic process of the surface reactions that generate H_2 and O_2. Thus, we do not explicitly model the photo-absorption event or the kinetic process of the subsequent charge migration. Photo-excitation and charge migration are considered to generate the electrochemical potentials for electrocatalytic H_2O decomposition.

4.1. Hydrogen evolution reaction on Ni_4O_2/β-$Ga_2O_3(100)$

HER involves binding of H atoms to the catalyst surface and recombinative desorption of molecular hydrogen, which plays an essential role in hydrogen fuel cells, electrodeposition, corrosion of metals and hydrogen energy storage.[62-64] These applications have led to a large body of research relevant to the HER, covering a broad range of systems including metals, alloys, hydrogenases, and semiconductors.[65-71] From these works, it has become evident that the HER activity can be correlated to the adsorption energy of a single H atom, that is to say, a good catalyst for the HER should exhibit a small adsorption energy for H ($|\Delta G_H| \approx 0$). In this work, we elucidate the thermochemistry of this reaction by computing the free energy of atomic hydrogen bonding to the clean Ga_2O_3 surface and Ni_4O_2/Ga_2O_3 surface, and comparing the hydrogen evolution activity of different sites. The free energy of the adsorbed state is calculated as

$$\Delta G_H = \Delta E_H + \Delta ZPE - T\Delta S_H \qquad (2)$$

where ΔE_H is the hydrogen chemisorption energy obtained from DFT calculations and

ΔZPE is the difference in zero point energy between the adsorbed and the gas phase. Since the vibrational entropy in the adsorbed state is small, the entropy of adsorption of 1/2 H_2 ΔS_H is approximately equal to the negative value of half the entropy of H_2 in the gas phase at standard conditions.

At first, we investigated the HER mechanism of clean β-Ga_2O_3(100) surface. As shown in our previous work,[30] the (100)-B surface of β-Ga_2O_3 is terminated by fivefold coordinated Ga and threefold coordinated O atoms. We considered surface O and Ga sites for hydrogen adsorption. The free energy of hydrogen adsorption ΔG_H on the O and Ga sites are predicted to be 0.47 and 2.45 eV, respectively. Based on the above discussion, one can see that if the $|\Delta G_H|$ is close to zero, the catalyst will be near its optimum performance composition. Therefore, the results indicate that O site is energetically more favorable than Ga site to occur HER. The free-energy diagram for hydrogen evolution at a potential U=0 relative to the standard hydrogen electrode at pH=0 is determined and shown in Fig. 4. As to Ni_4O_2/β-Ga_2O_3(100) surface, we initially examined all possible active sites for hydrogen adsorption, including O and Ni sites. Seven relaxed structures and the corresponding free energy changes of adsorption process are displayed in Fig. 4. The free-energy change of hydrogen adsorption reaction ΔG_H is predicted to be -0.29 eV for **O-1**, 0.13 eV for **O-2**, 0.66 eV for **O-3**, 0.76 eV for **O-4**, -0.31 eV for **Ni-1**, and -0.30 eV for **Ni-2**, 0.58 eV for **Ni-3**. The results indicate that **O-2** is the most favorable configuration for HER, which shows that the cluster oxygen atom is the most active site for the reaction. The Bader charge analysis above shows that cluster oxygen atoms have extra electrons, which

can transfer to the adsorbed hydrogen atoms to occur HER. **O-1**, **Ni-1** and **Ni-2** have similar stability, which are more favorable than clean Ga_2O_3 surface for HER. Generally, cluster oxygen atoms and Ni atoms in Ni_2 cluster are more active than surface oxygen atoms and Ni atoms in Ni_2O_2 clusters for HER. As shown in Fig. 4, adding Ni_4O_2 nanocluster can remarkably decrease the Gibbs free energy of HER, which may be one of the reasons that HER is experimentally promoted by loading NiO_x cocatalyst.

4.2. Water adsorption on surfaces

In photocatalytic applications, most reactions are carried out in aqueous solution or, at least, need the participation of water with surface hydroxyl radicals derived from water decomposition being an important reaction intermediate.[72,73] It is important to understand the interaction between water and semiconductor surfaces. Therefore, we investigated the adsorption of water and its dissociation on clean and modified Ga_2O_3 surfaces by Ni_4O_2 clusters. The bonding strength of water adsorption on surfaces can be calculated using the adsorption energy which was defined as

$$E_{ads} = E_{total} - E_{surf} - E_{H2O} \qquad (3)$$

in which E_{total} is the total energy of the water adsorbed surface after geometry relaxation, E_{surf} is the energy of the surface slab without water adsorption, E_{H2O} is the energy of one free water molecule. According to this definition, a more negative E_{ads} value corresponds to more exothermic and stronger adsorption. The following abbreviations are used in the text to describe the structure: O_s are the oxygen atoms in the exposed surface, Ga_s are gallium atoms in the topmost layer, O_w are the oxygen

atoms of water, and O_c are the oxygen atoms in Ni_4O_2 clusters.

We now start our discussion with the adsorption of a water molecule on clean β-Ga_2O_3(100) surface. As shown in Fig. 5(a), an isolated water molecule adsorbs to a surface gallium site through its O atom, with an adsorption energy of -0.57 eV. The plane of water molecule is nearly parallel to the surface. Water adsorption lifts up Ga_s slightly from the surface, and the Ga_s-O_w bond length is 2.159 Å. The average distance between H atoms and the nearest O_s atoms is 2.128 Å, which are short enough to generate hydrogen bonds to enhance the stability of the structure. We tried several starting configurations for dissociative adsorption of water. However, all the dissociatively adsorbed water ends up molecularly adsorption on the clean surface. In other words, our calculations indicate that molecular water adsorption on the clean β-Ga_2O_3(100) surface is energetically more favorable.

The most stable structure of Ni_4O_2/β-Ga_2O_3(100) in Fig. 1 was used to investigate the water adsorption. Nine stable geometries of the molecular water adsorption state are found and depicted in Fig. 5. The calculated adsorption energy ranges from -0.18 eV to -1.15 eV depending on the adsorbing site. For structure **b** and **c**, the O_w atom binds to a Ni atom and one of H atoms forms a hydrogen bond with O_c. Since the bond length of Ni-O_w and the distance between H1 and O_c in **c** are shorter than those in **b**, **c** is more stable than **b** by 0.25 eV. In configuration **d** and **e**, water molecule adsorbs to a Ga_s atom with the adsorption energy of -0.49 eV and -0.52 eV, respectively. The orientation of water on the surface is almost the same as that on the clean surface shown in Fig. 5(a). With respect to structure **f** and **g**, the O_w atom binds

to a Ni atom in Ni_2 segment and one H atom connects with one O_s atom through a hydrogen bond. The results show that the stability of adsorption structure is related to the strength of Ni-O_w bond (2.173 Å vs. 2.048 Å) and hydrogen bond (1.799 Å vs. 1.764 Å). In state **h** and **i**, the O_w atom forms a bond with a Ni atom in Ni_2O_2 segment and a hydrogen bond forms between one H atom and one O_c atom. The Ni-O_w bond length is 2.066 Å for **h** and 2.061 Å for **i**, and the distance of H-O_c bond is 1.992 Å for **h** and 1.819 Å for **i**. The shorter bond distance between water and Ni_4O_2 cluster results in the more stable structure. For the most stable structure **j**, the O_w atom forms a bond with a Ni atom in Ni_2O_2 moiety and an interfacial hydrogen bond forms between one H atom and one O_s atom. These results suggest that the strength of bonds formed between water molecule and Ni_4O_2 cluster/Ga_2O_3 surface is highly related to the stability of the adsorption structure.

Based on all of the molecular adsorption structures, we have relaxed as many as possible dissociative adsorption configurations and showed six stable structures in the bottom panels of Fig. 5. Our calculations indicate that the dissociative state of water adsorbed on Ga_s atom can't be found, as the case in clean surface. Structure **k** is the corresponding dissociative geometry of structure **f** and the former is energetically more favorable than the latter by 0.02 eV. As can be seen, water dissociates on the adjacent O_s site, leading to the formation of one Ga-O_w bond and breakage of one Ni-O_s bond. Direct transfer of one H atom in structure **h** to adjacent O_c atom generates configuration **l**, which makes one Ni-O_c bond broken. Structure **l** is more stable than **h** by 0.05 eV. The water dissociation in state **b** and **g** leads to the formation of structure

m with an adsorption energy of -1.26 eV. The hydroxyl group O_w-H in structure **m** binds to two Ni atoms, which stabilizes the system. The molecular water adsorbed state **c** is metastable to dissociated adsorption state **n**, and the energy difference between them is 0.83 eV. The dissociation of water in structure **i** generates configuration **o**, in which hydroxyl binds to a Ni atom and the dissociated H connects with an O_c atom. The adsorption energy of structure **o** is calculated to be -1.28 eV, which is lower than that of molecular adsorption state **i** by 0.44 eV. Taking the optimized molecular water adsorbed configuration **j** as the initial structure, we tried to find its dissociative modes. However, we cannot find the corresponding dissociative configuration with transferring the H atom pointing to the surface to the nearby O_s atom owing to the strong hydrogen bond. As a result, one dissociative adsorption structure **p** is found. The adsorption energy of this structure is 0.35 eV, which is more stable than the molecular adsorption structure **j** by 0.19 eV. In mode **p**, O_w-H is attached to a Ni atom and one of H atoms transfers to an adjacent O_c atom to form a new O-H bond. The results above suggest that dissociation of water tends to occur on the Ni_4O_2 cluster rather than on the interface between the cluster and Ga_2O_3 surface.

4.3. Oxygen evolution reaction

In the overall water splitting reaction, OER is considered to be more difficult than HER because the former involves a four-electron-transfer process. The mechanism of OER is complicated and not fully established yet. Insights into the thermodynamics of the reaction can be obtained using the scheme developed by Nørskov and co-workers,[74-76] where the molecular oxygen is formed via a surface HOO*

intermediate and the reaction takes place at the coordinatively unsaturated surface sites. In this scheme, OER is assumed to consist of four elementary reaction step, each involving the electron transfer accompanied by proton removal:

$$H_2O + * \rightarrow HO* + H^+ + e^- \quad (A)$$

$$HO* \rightarrow O* + H^+ + e^- \quad (B)$$

$$O* + H_2O \rightarrow HOO* + H^+ + e^- \quad (C)$$

$$HOO* \rightarrow * + O_2 + H^+ + e^- \quad (D)$$

where * denotes a surface site and X* represents an adsorbed X intermediate on the surface. We obtain the energy of $H^+ + e^-$ implicitly by referencing it to the energy of H_2 using the standard hydrogen electrode. This implies that at standard conditions (pH=0, p=1 bar and T=298 K) the free energy of $H^+ + e^-$ can be taken equal to be half the formation energy of H_2. The reaction free energy, $\Delta G=\Delta E+\Delta ZPE-T\Delta S$, is calculated as follows: The reaction energy ΔE is obtained from DFT calculations. ΔZPE and ΔS are calculated using computed vibrational frequencies and standard tables for the reactants and products in the gas phase.[64] The entropies for the atoms and molecules adsorbed to the surface active site are assumed to be zero. The temperature dependence of the enthalpy is neglected in these calculations. Applying an external bias U on each proton-coupled electron transfer step is accounted for by including a $-eU$ term in the reaction free energy. For simplicity, the effect of pH is not considered here and we restrict the calculations to pH=0. Therefore, the reaction free energies are expressed as follows:

$$\Delta G_A = E(HO*) - E_{H_2O} + 1/2\, E_{H_2} + (\Delta ZPE - T\Delta S)_A - eU \quad (4)$$

$$\Delta G_B = E(O^*) - E(HO^*) + 1/2\, E_{H_2} + (\Delta ZPE - T\Delta S)_B - eU \quad (5)$$

$$\Delta G_C = E(HOO^*) - E(O^*) - E_{H_2O} + 1/2\, E_{H_2} + (\Delta ZPE - T\Delta S)_C - eU \quad (6)$$

$$\Delta G_D = E(^*) - E(HOO^*) + E_{O_2} + 1/2 E_{H_2} + (\Delta ZPE - T\Delta S)_D - eU \quad (7)$$

where $E(^*)$, $E(HO^*)$, $E(O^*)$ and $E(HOO^*)$ are the calculated DFT energies of the clean surface and surfaces with adsorbed HO*, O* and HOO*, respectively. E_{H_2O}, E_{H_2} and E_{O_2} are the calculated energies for the isolated gaseous molecules H_2O, H_2 and O_2, respectively. The free-energy change of the total reaction $H_2O \rightarrow 1/2\ O_2 + H_2$ is fixed at the experimental value of 2.46 eV per water molecule. This means that in the reaction step involving the formation of O_2, we consider that $\Delta G_{(2H_2O \rightarrow O_2 + 2H_2)} = 4.92$ eV $= E_{O_2} + 2E_{H_2} - 2E_{H_2O} + (\Delta ZPE\text{-}T\Delta S)_{(2H_2O \rightarrow O_2 + 2H_2)}$. The reaction overpotential can be calculated from the difference between the voltage at which all free-energy steps become downhill and the minimum voltage required for the OER.

Fig. 6 shows the calculated free energy diagrams of OER on the clean $Ga_2O_3(100)$, and Ni_4O_2/Ga_2O_3 surfaces at pH = 0, T = 298 K and different biases, and the relaxed structures of intermediates. The computed results demonstrate that, for no applied bias, U = 0 V, all steps in all the surfaces are uphill. Even at standard equilibrium potential for oxygen evolution at U = 1.23 V, some of the steps become downhill but some still remain uphill. So it is necessary to impose a bias (or overpotential) on both surfaces to have every step downhill. As shown in Fig 6(a), for the clean Ga_2O_3 surface, the rate limiting step is the first step, the process of generating the OH* species, because the water dissociation is very difficult. The overpotential needed in the clean surface is 1.34 V (= 2.57 – 1.23 V). To investigate the effect of water phase around the reaction

center, we considered a situation when a water layer placed on the clean surface. The rate-determining step is also the first step and the calculated overpotential is 1.32 V, which are very similar to the surface with water monomer. After adsorbing Ni_4O_2 cluster onto the Ga_2O_3 surface, the calculated overpotential remarkably decreases. The value of overpotential is 0.47 V (= 1.71 – 1.23 V). With respect to Ni_4O_2/Ga_2O_3 surface, the second step becomes the rate determining step as depicted in Fig. 6(b), in which a proton is transferred from the adsorbed OH* species to the electrolyte. The notable reduction of overpotential (0.87 V) for OER on Ni_4O_2/Ga_2O_3 is found compared with that on clean Ga_2O_3 surface, which explains the experimental observation on significant enhancement of activity for generating oxygen after loading NiO_x cocatalysts.

Conclusions

We performed a detailed investigation on the water adsorption and mechanism of water-splitting reaction on NiO_x/β-Ga_2O_3 system by means of first-principles DFT calculations. The conclusions are as follows:

(1) The most favorable structure of Ni_4O_2/β-$Ga_2O_3(100)$ is composed of the most stable structures of Ni_2/β-$Ga_2O_3(100)$ and Ni_2O_2/β-$Ga_2O_3(100)$ with some distortions. The formation of NiO_x on Ga_2O_3 surface is predicted to be energetically favorable.

(2) In Ni_4O_2/β-$Ga_2O_3(100)$ system, cluster oxygen atoms and Ni atoms in Ni_2 cluster are more active than surface oxygen atoms and Ni atoms in Ni_2O_2 clusters for HER. Loading Ni_4O_2 nanocluster on Ga_2O_3 surface can remarkably decrease the

Gibbs free energy of HER.

(3) On the basis of the computed adsorption energies, it is found that water dissociation is energetically unfavorable on the clean β-Ga_2O_3(100) surface. The addition of Ni_4O_2 cluster makes the decomposition process favorable. Dissociation of water tends to occur on the Ni_4O_2 cluster rather than the interface between cluster and the Ga_2O_3 surface.

(4) The strength of hydrogen bond formed between water and Ni_4O_2/Ga_2O_3 surface is highly related to the stability of the adsorption structure.

(5) The overpotential needed for OER on Ni_4O_2/Ga_2O_3 is calculated to be lower than that on clean Ga_2O_3 surface by 0.87 V.

(6) Our theoretical findings provide reasonable explanations on the experimentally significant enhancement of activity for photocatalytic water-splitting reaction after loading NiO_x cocatalysts.

Acknowledgements

This work is financially supported by National Natural Science Foundation of China under Grant 21473183 and 21303079.

References

1 S. Y. Reece, J. A. Hamel, K. Sung, T. D. Jarvi, A. J. Esswein, J. J. H. Pijpers and D. G. Nocera, *Science*, 2011, **334**, 645-648.

2 K. Maeda, K. Teramura, D. L. Lu, T. Takata, N. Saito, Y. Inoue and K. Domen, *Nature*, 2006, **440**, 295-295.

3 A. Kudo and Y. Miseki, *Chem. Soc. Rev.* 2009, **38**, 253-278.

4 X. Chen, S. Shen, L. Guo and S. S. Mao, *Chem. Rev.* 2010, **110**, 6503-6570.

5 A. Fujishima and K. Honda, *Nature*, 1972, **238**, 37-38.

6 J. Yang, D. Wang, H. Han and C. Li, *Acc. Chem. Res.*, 2013, **46**, 1900-1909.

7 X. Zong, H. J. Yan, G. P. Wu, G. J. Ma, F. Y. Wen, L. Wang and C. Li, *J. Am. Chem. Soc.*, 2008, **130**, 7176-7177.

8 H. Yan, J. Yang, G. Ma, G. Wu, X. Zong, Z. Lei, J. Shi and C. Li, *J. Catal.*, 2009, **266**, 165-168.

9 D. Y. C. Leung, X. L. Fu, C. F. Wang, M. Ni, M. K. H. Leung, X. X. Wang and X. Z. Fu, *ChemSusChem,* 2010, **3**, 681-694.

10 D. Wang, R. Li, J. Zhu, J. Shi, J. Han, X. Zong and C. Li, *J. Phys. Chem. C*, 2012, **116**, 5082-5089.

11 K. S. S. Ma, K. Maeda, R. Abe and K. Domen, *Energy Environ. Sci.*, 2012, **5**, 8390-8397.

12 M. Higashi, K. Domen and R. Abe, *J. Am. Chem. Soc.*, 2012, **134**, 6968-6971.

13 F. E. Osterloh, *Chem. Mater.*, 2008, **20**, 35-54.

14 T. Yanagida, Y. Sakata and H. Imamura, *Chem. Lett.*, 2004, **33**, 726-727.

15 Y. Sakata, Y. Matsuda, T. Yanagida, K. Hirata, H. Imamura, K. Teramura, *Catal. Lett.*, 2008, **125**, 22-26.

16 X. Wang, Q. Xu, M. Li, S. Shen, X. Wang, Y. Wang, Z. Feng, J. Shi, H. Han and C. Li, *Angew.Chem. Int. Ed.* 2012, **51**, 13089-13092.

17 X. Wang, S. Shen, S. Jin, J. Yang, M. Li, X. Wang, H. Han, C. Li, *Phys. Chem. Chem. Phys.*, 2013, **15**, 19380-19386.

18 Y. Sakata, T. Nakagawa, Y. Nagamatsu, Y. Matsuda, R. Yasunaga, E. Nakao, H. Imamura, *J. Catal.*, 2014, **310**, 45-50.

19 H. Kato, K. Asakura and A. Kudo, *J. Am. Chem. Soc.*, 2003, **125**, 3082-3089.

20 T. K. Townsend, N. D. Browning and F. E. Osterloh, *Energy Environ. Sci.*, 2012, **5**, 9543-9550.

21 K. Maeda, K. Teramura, D. Lu, N. Saito, Y. Inoue and K. Domen *Angew. Chem. Int. Ed.* 2006, **45**, 7806-7809.

22 D. Matthey, J. G. Wang, S. Wendt, J. Matthiesen, R. Schaub, E. Laegsgaard, B. Hammer and F. Besenbacher, *Science*, 2007, **315**, 1692-1696.

23 H. G. Yang, C. H. Sun, S. Z. Qiao, J. Zou, G. Liu, S. C. Smith, H. M. Cheng and G. Q. Lu, *Nature*, 2008, **453**, 638-641.

24 Y. Pan, C. Liu, Q. Ge, *J. Catal.*, 2010, **272**, 227-234.

25 Y.-F. Li, Z.-P. Liu, L. L. Liu and W. Gao, *J. Am. Chem. Soc.*, 2010, **132**, 13008- 13015.

26 E. Escamilla-Roa, V. Timon, A. Hernandez-Laguna, *Comput. Theo. Chem.*, 2012, **981**, 59-67.

27 M. Setvin, U. Aschauer, P. Scheiber, Y.-F. Li, W. Hou, M. Schmid, A. Selloni and U. Diebold, *Science*, 2013, **341**, 988-991.

28 M. Zhang, J. Chen, Y. Yu and Y. Zhang, *Appl. Surf. Sci.*, 2013, **287**, 97-107.

29 J. Li, E. Croiset, L. Ricardez-Sandoval, *J. Phys. Chem. C*, 2013, **117**, 16907-16920.

30 T. Liu, I. Tranca, J. Yang, X. Zhou, C. Li, *J. Mater. Chem. A*, 2015, **3**, 10309-10319.

31 G. Kresse and J.Furthmüller, *Phys. Rev. B,* 1996, **54**, 11169.

32 G. Kresse and J.Furthmüller, *Comput. Mater. Sci.*, 1996, **6**, 15-50.

33 J. P. Perdew, K. Burke and M.Ernzerhof, *Phys. Rev. Lett.*, 1996, **77**, 3865-3868.

34 P. E. Blochl, *Phys. Rev. B,* 1994, **50**, 17953-17979.

35 G. Kresse and J. Joubert, *Phys. Rev. B*, 1999, **59**, 1758-1775.

36 S. L. Dudarev, G. A. Botton, S. Y. Savrasov, C. J. Humphreys and A. P. Sutton, *Phys. Rev. B*,

1998, **57**, 1505-1509.

37 A. M. Ferrari, C. Pisani, F. Cinquini, L. Giordano and G. Pacchioni, *J. Chem. Phys.*, 2007, **127**, 174711.

38 W. E. Pickett, S. C. Erwin and E. C. Ethridge, *Phys. Rev. B*, 1998, **58**, 1201-1209.

39 O. Bengone, M. Alouani, P. Blöchl and J. Hugel, *Phys. Rev. B*, 2000, **62**, 16392- 16401.

40 J. Heyd, G. E. Scuseria and M. Ernzerhof, *J. Chem. Phys.*, 2003, **118**, 8207-8215.

41 J. Heyd, G. E. Scuseria and M. Ernzerhof, *J. Chem. Phys.*, 2004, **121**,1187-1192.

42 J. Heyd, G. E. Scuseria and M. Ernzerhof, *J. Chem. Phys.*, 2006, **124**, 219906.

43 M. Cococcioni and S. de Gironcoli, *Phys. Rev. B*, 2005, **71**, 035105.

44 A. E. Raeber and B. M. Wong, *J. Chem. Theory Comput.*, 2015, **11**, 2199-2209.

45 R. Roy, V. G. Hill and E. F. Osborn, *J. Am. Chem. Soc.*, 1952, **74**, 719-722.

46 B. Zheng, W. Hua, Y. Yue and Z. Gao, *J. Catal.*, 2005, **232**, 143-151.

47 Y. Hou, L. Wu, X. Wang, Z. Ding, Z. Li and X. Fu, *J. Catal.*, 2007, **250**, 12-18.

48 H. He, R. Orlando, M. A. Blanco, R. Pandey, E. Amzallag, I. Baraille and M. Rérat, *Phys. Rev. B*, 2006, **74**, 195123.

49 S. Yoshioka, H. Hayashi, A. Kuwabara, F. Oba, K. Matsunaga and I. Tanaka, *J. Phys.: Condens. Matter*, 2007, **19**, 346211.

50 Y. Sakata, Y. Matsuda, T. Yanagida, K. Hirata, H. Imamura and K. Teramura. *Catal. Lett.*, 2008, **125**, 22-26.

51 T. C. Lovejoy, E. N. Yitamben, N. Shamir, J. Morales, E. G. Villora, K. Shimamura, S. Zheng, F. S. Ohuchi and M. A. Olmstead, *Appl. Phys. Lett.*, 2009, **94**, 081906-1-3.

52 Y. Hou, J. Zhang, Z. Ding and L. Wu, *Powder Technol.*, 2010, **203**, 440-446.

53 Y. Sakata, Y. Matsuda, T. Nakagawa, R. Yasunaga, H. Imamura and K. Teramura, *ChemSusChem*, 2011, **4**, 181-184.

54 T. Oshima, K. Kaminaga, H. Mashiko, A. Mukai, K. Sasak, T. Masui, A. Kuramata, S.Yamakoshi, and A. Ohtomo., *Jpn. J. Appl. Phys.* 2013, **52**, 111102.

55 S. Geller, *J. Chem. Phys.,* 1960, **33**, 676.

56 V. M. Bermudez, *Chem. Phys.*, 2006, **323**, 193-203.

57 Y. Tomm, P. Reiche, D. Klimm and T. Fukuda, *J. Cryst. Growth*, 2000, **220**, 510-514.

58 E. G. Villora, Y. Murakami, T. Sugawara, T. Atou, M. Kikuchi, D. Shindo and T. Fukuda, *Mater. Res. Bull.*, 2002, **37**, 769-774.

59 H. H. Tippins, *Phys. Rev. A*, 1965, 140, A316-A319.

60 N. Ueda, H. Hosono, R. Waseda and H. Kawazoe, *Appl. Phys. Lett.*, 1997, 71, 933- 935.

61 W. Gao, J. E. Mueller, J. Anton, Q. Jiang and T. Jacob, *Angew. Chem. Int. Ed.*, 2013, **52**, 14237-14241.

62 M. Z. Jacobson, W. G.Colella and D. M. Golden, *Science*, 2005, **308**, 1901-1905.

63 C. H. Hamann, A.Hamnett and W.Vielstich, *Electrochemistry*, Wiley-VCH, Weinheim, **1998**.

64 D. R. Lide, *CRC Handbook of Chemistry and Physics*, 84thed; CRC Press: Boca Raton, FL, 2003-2004.

65 J. K. Nørskov, T. Bligaard, A.Logadottir, J. R.Kitchin, J. G. Chen, S.Pandelov and U.Stimming, *J. Electrochem. Soc.,* 2005, **152**, J23-J26.

66 B. Hinnemann, P. G. Moses, J.Bonde, K. P.Jørgensen, J. H. Nielsen, S.Horch, I.Chorkendorff and J. K.Nøvskov, *J. Am. Chem. Soc*., 2005, **127**, 5308-5309.

67 J. Greeley, J. K.Nørskov, L. A.Kibler, A. M. El-Aziz and D. M. Kolb, *ChemPhysChem,* 2006, **7**,

1032-1035.

68 P. Liu and J. A. Rodriguez, *J. Am. Chem. Soc.,* 2005, **127**, 14871-14878.

69 J. Greeley, T. F. Jaramillo, J.Bonde, I.Chorkendorff and J. K.Nørskov, *Nat. Mater.,* 2006, **5**, 909-913.

70 J. Greeley and J. K.Nørskov, *Surf. Sci.,* 2007, **601**, 1590-1598.

71 E. Santos, P.Quaino and W.Schmickler, *Phys. Chem. Chem. Phys.,* 2012, **14**, 11224-11233.

72 M. A. Fox and M. T.Dulay, *Chem. Rev*., 1993, **93**, 341-357.

73 M. R. Hoffmann, S. T. Martin, W. Choi and D. W.Bahnemann, *Chem. Rev*., 1995, **95**, 69-96.

74 J. Rossmeisl, Z.-W. Qu, H. Zhu, G.-J. Kroes, and J. K. Nørskov, *J. Electroanal. Chem.*, 2007, **607**, 83-89.

75 Á. Valdés, Z.-W.Qu, G.-J.Kroes, J.Rossmeisl and J. K. Nørskov, *J. Phys. Chem. C,* 2008, **112**, 9872-9879.

76 I. C. Man, H.-Y. Su, F. Calle-Vallejo, H. A. Hansen, J. I. Martínez, N. G. Inoglu, J. Kitchin, T. F. Jaramillo, J. K.Nørskov and J. Rossmeisl, *ChemCatChem,* 2011, **3**, 1159-1165.

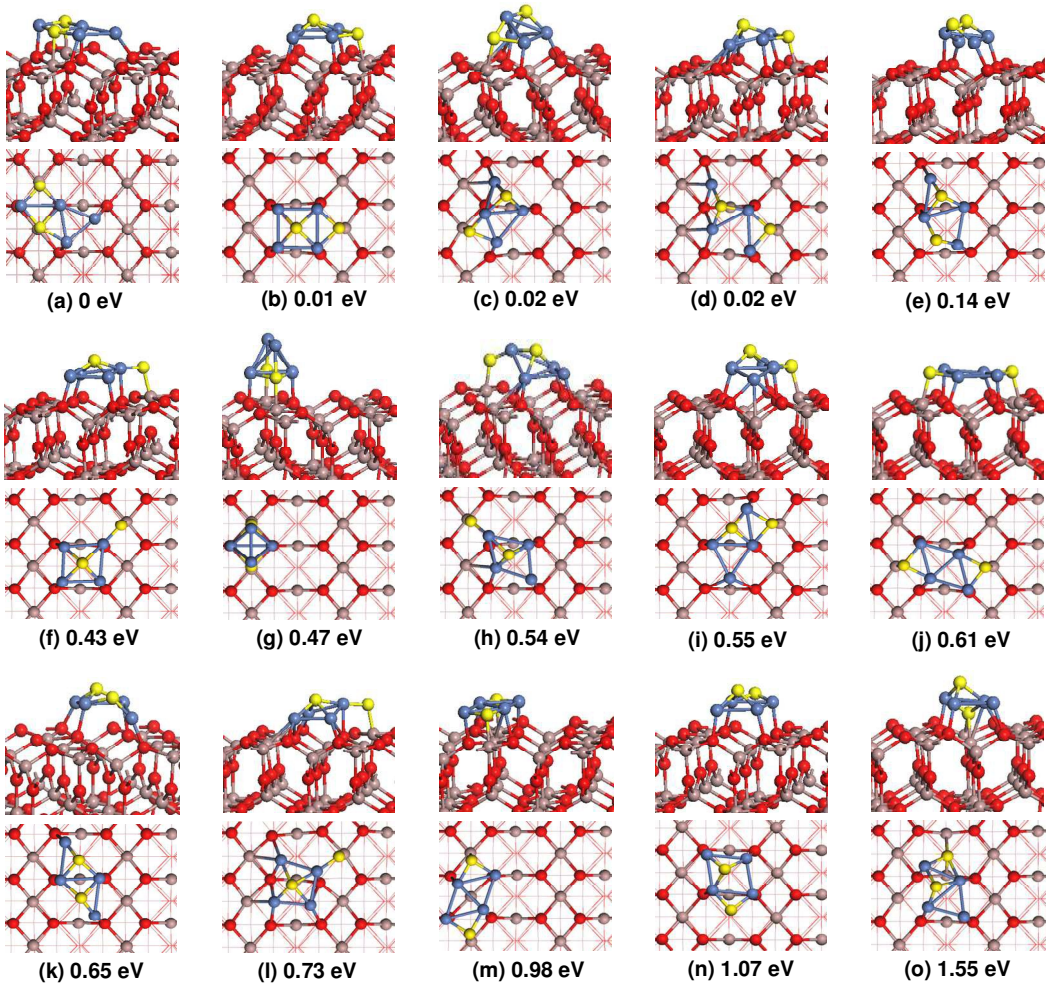

Fig.1 Optimized structures for the supported Ni_4O_2 cluster on the β-Ga_2O_3(100) surface (side and top views). Relative energies with respect to the corresponding lowest-energy structure are shown. Coloring scheme: red (surface O), brown (Ga), yellow (adsorbed O) and blue (Ni).

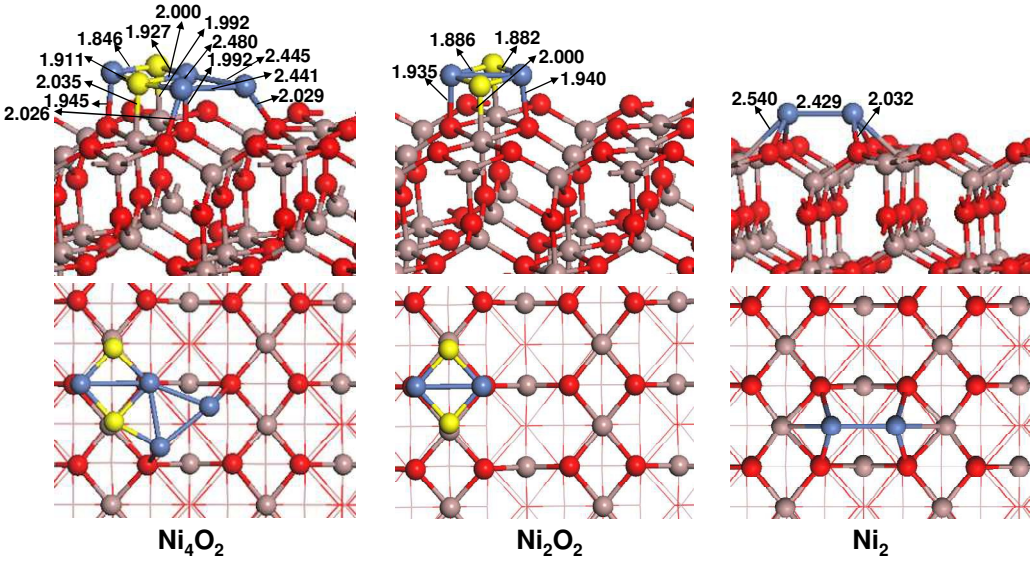

Fig. 2 Geometrical parameters of the most stable structure for the supported Ni_4O_2, Ni_2O_2 and Ni_2 cluster on β-Ga_2O_3(100) surface. Coloring scheme: red (surface O), brown (Ga), yellow (adsorbed O) and blue (Ni).

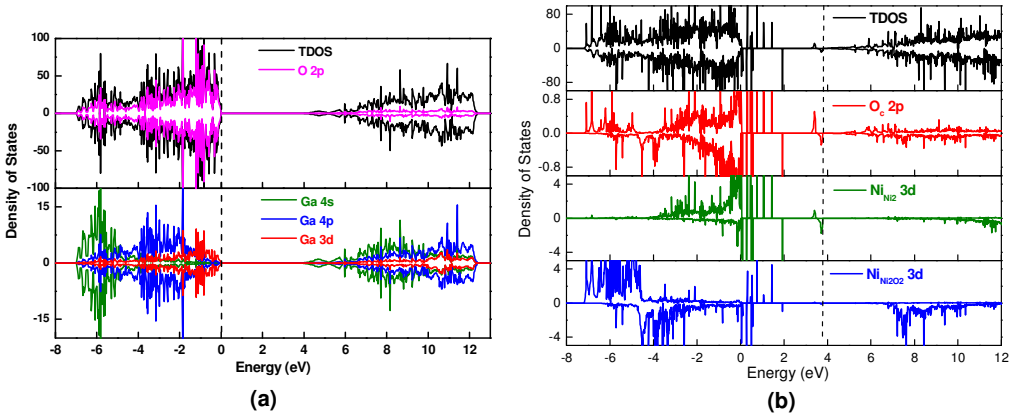

Fig. 3 Density of states for clean $Ga_2O_3(100)$ and Ni_4O_2/Ga_2O_3 surfaces. The Fermi level is shown the by the vertical dashed line.

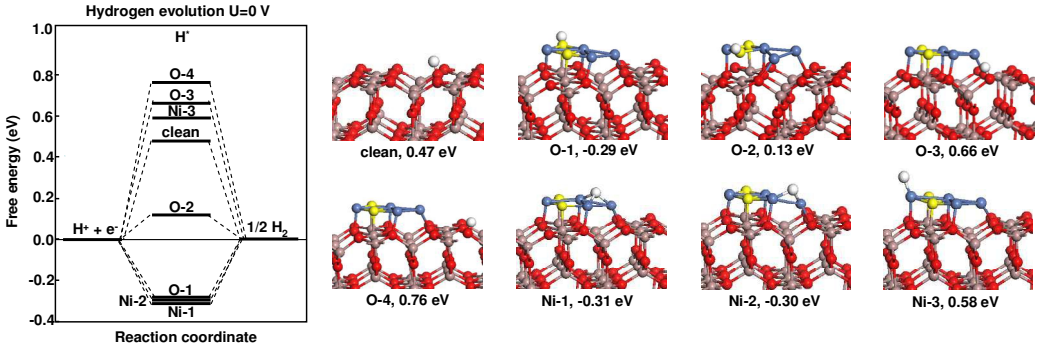

Fig. 4 Calculated free-energy diagram for hydrogen evolution at a potential U=0 relative to the standard hydrogen electrode at pH=0. Relaxed structures for H adsorbed clean $Ga_2O_3(100)$ and Ni_4O_2/Ga_2O_3 surfaces and the corresponding computed free energy of hydrogen adsorption reaction. Coloring scheme: red (surface O), brown (Ga), yellow (adsorbed O), blue (Ni) and white (H).

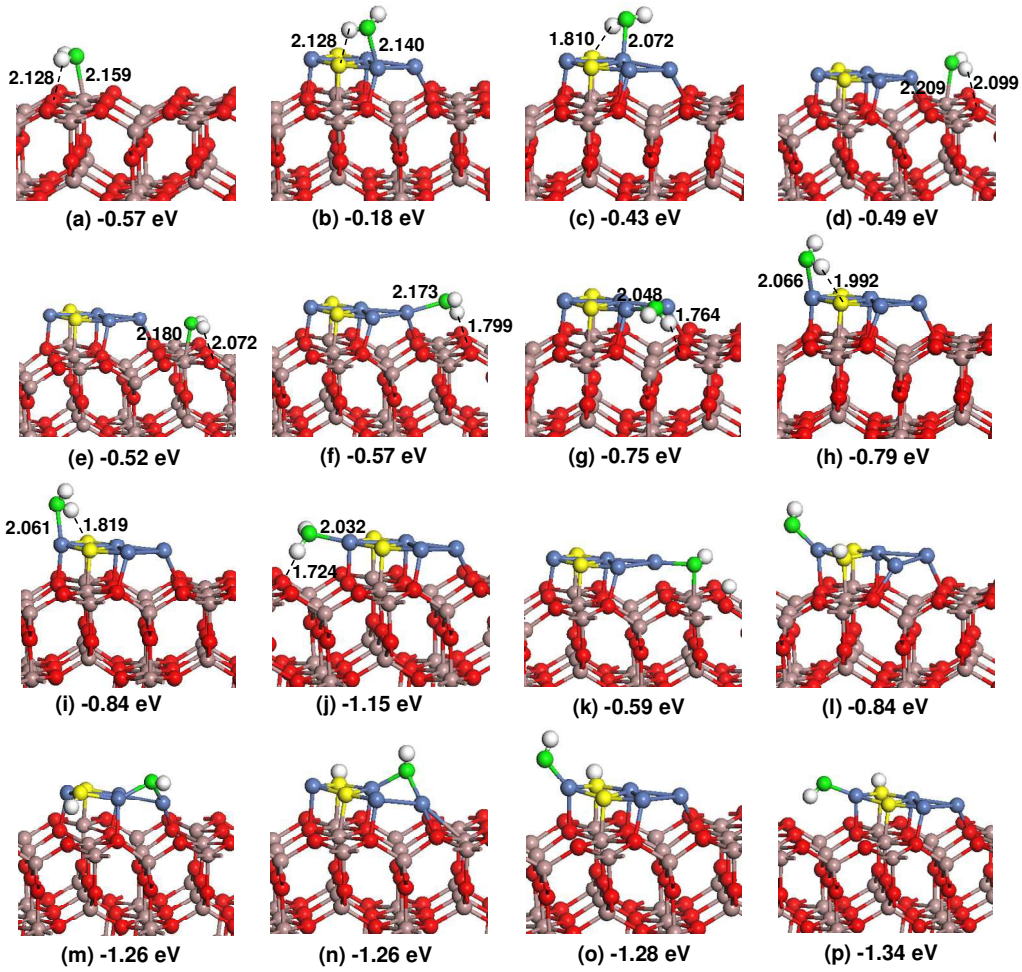

Fig. 5 Optimized structures of water molecular and dissociative adsorption on clean $Ga_2O_3(100)$ and Ni_4O_2/Ga_2O_3 surfaces. The computed adsorption energies are shown under the corresponding structures. Coloring scheme: red (surface O), brown (Ga), yellow (adsorbed O), blue (Ni), green (O from water) and white (H).

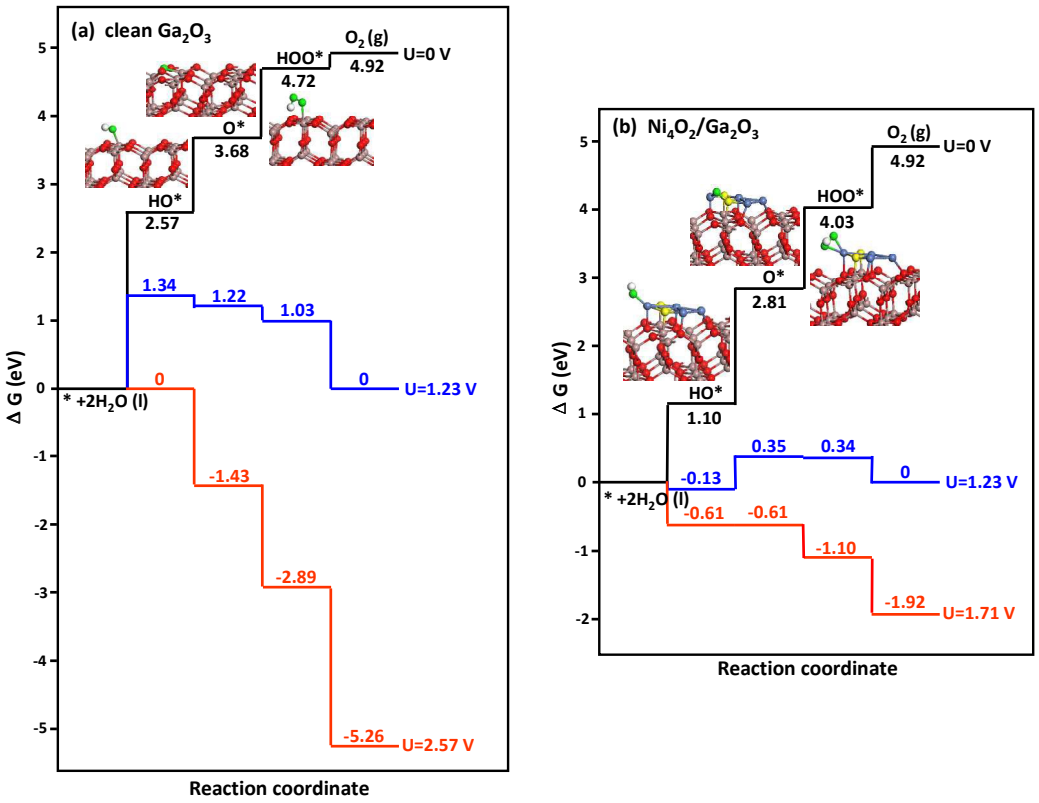

Fig. 6 Free energy diagrams at pH=0 and T=298 K for four steps of OER at different applied potentials for clean Ga_2O_3(100) and Ni_4O_2/Ga_2O_3 surfaces. Coloring scheme: red (surface O), brown (Ga), yellow (adsorbed O), blue (Ni), green (O from water) and white (H).